

Method and Design of an Autonomous In-Space Truss Assembly Robot

John E. Cross* and Spencer Cornwell†
University of Texas at Arlington, Arlington, Texas, 76010

Juan D. Rodriguez‡
University of Texas at Arlington, Arlington, Texas, 76010

Nevin Puthenpurackal§
University of Texas at Arlington, Arlington, Texas, 76010

Nicholas Hermes¶
University of Texas at Arlington, Arlington, Texas, 76010

This project is an entry to the COSMIC Capstone Challenge, where students design a conceptual payload to advance the nations In-space Servicing, Assembly, and Manufacturing (ISAM) capabilities. The challenge requires participants to “design a payload, to be hosted about the BCT X-Sat Venus Class bus, that will demonstrate a chain of 3 or more operations that provide an on-orbit, autonomous ISAM capability.” Through trade studies and research, our team identified the need for autonomous truss assembly to enable scalable, hands-off construction of space structures, enhancing mission flexibility. In response, we propose a robotic system that autonomously assembles modular trusses using thermoplastic induction welding. The robot employs a novel locomotion method, pivoting around truss nodes to navigate and construct efficiently. This system reduces reliance on crewed intervention, enabling the rapid deployment of large-scale orbital structures and paving the way for the future of mankind’s space exploration.

I. Nomenclature

T	=	torque
I	=	moment of inertia
α	=	angular acceleration
T_G	=	torque on gear
T_P	=	torque on pinion
N_G	=	number of gear teeth
N_P	=	number of pinion teeth

II. Introduction

A. Problem Statement

The challenge presented by the Consortium for Space Mobility and ISAM Capabilities (COSMIC) to develop a conceptual design that is able demonstrate one or multiple ISAM capabilities, having been launched with a Blue Canyon Technologies Venus-class bus. ISAM capabilities include servicing vehicles, assembly of structures, or manufacturing

*Team Lead

†CAD and Manufacturing

‡CAD and Manufacturing

§Documentation

¶Documentation

in space. The capability we chose must comprise of at least three operations in sequence. An operation is any action performed by a device, such as polymer extrusion, moving a part, or generating a signal.

B. Motivation

Development of Space Mobility technologies and ISAM technologies has been identified by the United States government as an important part of maintaining its technological lead in space exploration and national security. Through the Consortium of Space Mobility and ISAM Capabilities, a cooperation between NASA and the private space sector, the C3 competition aims to promote the generation of concepts for in-space servicing, assembly, and manufacturing for future space missions.

A major challenge to current ISAM capabilities is the difficulty of building large structures in-situ. This difficulty is well illustrated by the development of the International Space Station, which in early concepts involved the assembly of a sprawling orbital complex including large external trusses built as an environment for orbital assembly and research. In the final design, due to the impracticality of orbital construction work, this truss survived as a much smaller structure assembled from large components prefabricated on Earth. This project seeks to innovate orbital construction by providing the design for a spacecraft capable of constructing planar trusses from small, packed parts with minimal human supervision.

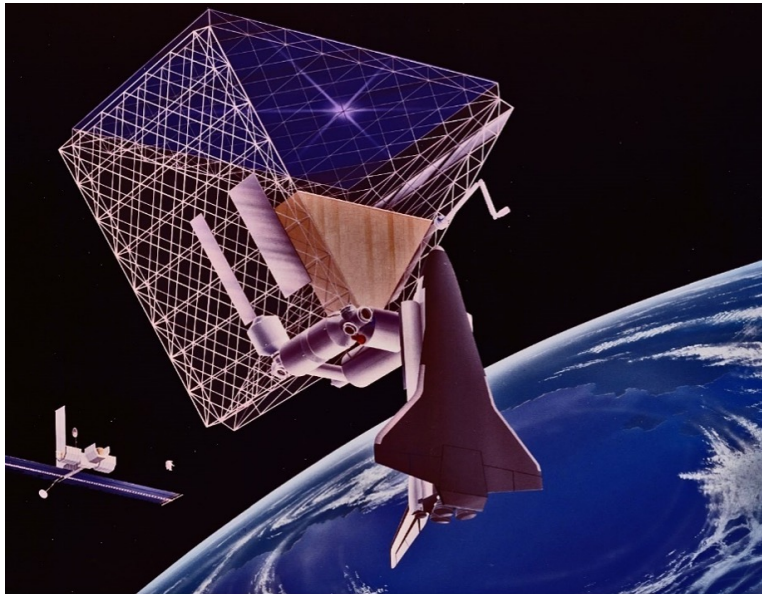


Fig. 1 Space construction yard concept [1]

C. Trade Studies and Background Research

As the problem given is broad and abstract, a large portion of time and effort was dedicated to educating the team on the conditions of space and demand for different ISAM capabilities. This was all in effort to educate the decision of what mission we will be tackling.

1. Launch and Sub Orbital Conditions

The conditions for launch are generally described in the payload user's guide for the rocket on which the spacecraft is to launch. The mission has been assumed to launch as a ride-along payload on the ubiquitous SpaceX Falcon-9 launch vehicle. The SpaceX rideshare guide provides a description of the requirements and conditions for launch. These include the expected quasi-static g-loading, acoustic vibrations, and electrical emission restrictions[2]. the environmental conditions in sub orbital space flight are continuously changing. Acoustic and structural vibrations during launch from exhaust gases can compromise the structural integrity of the payload and must be carefully analyzed during the design process [3]. The payload is also subject to temperatures ranging between 26 °C and 49 °C during a

suborbital flight [3]. On the other hand, the radiation environment up to an altitude of 90 km is relatively stable.[3].

2. *Environment in Orbit*

We have been given ample discretion on what ISAM technology to use, where it will operate, and what purpose it will serve. Trade studies began by identifying the different environments our concept could face. These include low Earth orbit (LEO), geostationary Earth orbit (GEO), and cislunar space, often called extended geostationary orbit (xGEO) all of which have a varying degree of environmental conditions. In addition to the multitude of challenges within the different orbital levels, we also needed to educate ourselves on the different operations that would even be performed in separate orbital levels.

Low Earth orbit is defined as being up to 2,000 km from the Earth's surface. As of 2022, there are over 4,500 active satellites in LEO. Satellites in LEO have short lag times, so they are commonly used for communications to and from the ground [4]. Operating in a geostationary orbit consists of a body moving in sync with the earth's rotation. GEO occurs above the equator at approximately 36,000 km above the Earth's surface [5]. Cislunar space is the space "higher" than geostationary orbit but within the sphere of influence of the Earth; xGEO is higher than 36,000 km above sea level, but below the orbital height of the moon and can contain orbits of different inclinations. The xGEO belt is often used for operations such as weather monitoring and communication relays. This is similar to the GEO belt, however it does not include the equatorial restriction. This allows the benefit of greater coverage of the Earth as well as avoiding heavier satellite traffic. These benefits come at the cost of the energy required to reach this belt and increased levels of propulsion technology and orbital planning.

Present in all orbital levels discussed are debris, radiation, thermal cycling, and cold welding. There is an estimated 25,000 pieces of debris larger than 100 mm in LEO, however, the debris which poses the greatest threat is between 5 to 100 mm in size. This debris is dangerous because it can cause significant damage but is difficult for satellites to detect [4]. A challenge particular to cislunar space regarding debris is the difficulty to predict behavior of the Earth-Moon dynamic system [6]. Harmful radiation, mostly in the form of solar flares and coronal mass ejections, have the potential to cause permanent damage to critical electrical systems aboard satellites [7]. For deep space applications, satellites are designed with advanced shielding and logical redundancies [8]. The thermal challenge when in xGEO is less demanding than lower orbits as it does not have the quick temperature fluctuations and for this reason can be considered with less worry. In LEO, the temperatures range from -65 °C to 125 °C, with the number of cycles ranging from 6,000 to 20,000 depending on the orbital height [9]. Direct metal to metal contact between moving surfaces can cause cold welding to occur. This happens because there is no atmosphere preventing these surfaces from bonding [10].

3. *Other Considered ISAM Technologies*

The early to middle stages of this portion of the project were centered around research and defining the capabilities we wanted to pursue. To that end, numerous possible ISAM capabilities were explored and weighed. Ultimately five technologies stood out as being potentially in-scope and worthy of pursuit. These were the ultimately selected truss assembly, as well as computed axial lithography, solar panel repair, manual satellite stabilization, and debris recycling.

Computed axial lithography is a recently developed additive manufacture technique based on the projection of a rotating image of the desired design onto a rotating volume of photopolymer liquid. This allows for the rapid printing of 3D shapes without the need for a flat liquid-gas interface, and also permitting the addition of inclusions within the printed models [11]. Although this method was found to be interesting and worthwhile, it was already being researched. It was also found to be beyond our capabilities to build a meaningful prototype.

Solar panel repair drew interest as a potential method of extending satellite lifetime. Ultimately the team was unable to determine a favored approach between direct repair, refurbishment, or replacement, which left this possibility to lose traction to alternatives with broader applications or more concrete methods.

Manual satellite stabilization was focused on the construction of a spacecraft capable of rendezvous with a rotating object in orbit, either a large piece of space debris or an uncontrolled satellite. After rendezvous, this satellite would be capable of connecting to that object and arresting its rotation. This would provide an opportunity to send more spacecraft to either service or deorbit the object. Both destructive and non-destructive methods of connection were considered. Ultimately this option was not selected on account of its difficulty and its questionable applications at scale.

Debris recycling was focused on the collection of space debris and its possible use in the space industry, especially in additive manufacturing. Initially this focused on the collection and repurposing of small debris, however this proved impractical due to the difficulty of collecting small debris in an environment as large as LEO. A refocus on large debris showed a paucity of targets in useful orbits, as the vast majority of large debris items lie in near-polar orbits [12]. A final

refocus on the usability of already collected small debris left this capability in such a restricted niche as to be largely pointless to pursue.

III. Design

A. Constraints and Specifications

This design is intended to be a payload onboard the X-Sat Venus class satellite bus by Blue Canyon Technologies. Therefore, the design is limited to fit within a volume of 40 gallons (20.5" x 16.4" x 27.0") for a power output of 222W or 32 gallons (17.0" x 16.4" x 27") for a power output of 444W. The design must survive launch and the orbital environment.

For the current design, the specifications are listed:

- 266 W pancake induction coil
- x2 15 W brushless motors
- x3 10.8 W brushless motors
- x4 servo motors, low power
- Total mass: 17 kg (for all materials being 2024-T3 aluminum)
- Compressed volume 628mm x 180mm x 303mm

B. Additional Research

After the concept selection process was completed, we began to brainstorm ideas on how to build trusses and how the different components will be affected by the space environment. The team needed to define what material was appropriate to use for the truss, how to deal with sliding friction in space, and what joining techniques work.

1. Friction and Lubrication in Space

Building trusses in space requires the use of actuators and mechanisms to manipulate truss elements and join them. One of the first obstacles the team came across was the cold welding of metals in space. In the absence of an atmosphere, sliding between metal surfaces causes the metal surfaces to fuse resulting in increased friction. A larger power draw from the actuator motors results from the increased friction until the mechanism completely fails. To prevent this or slow down the rate of wear solid lubricants and greases are used.

The John Hopkins University Applied Physics Laboratory has conducted multiple experiments with different types of lubricants under different load conditions. In a summary report of the results of these experiments, it was recommended to use Teflon, Molybdenum Sulfide, graphite, or tri-crestyl phosphate for high load applications. These are burnished or deposited onto surfaces. These lubricants work themselves into imperfections in the surfaces and create a solid film. Teflon and Molybdenum Sulfide are also used as high pressure grease additives for gears [13].

Sealing in the power transmission mechanism is also important to prevent contaminants from entering and prevent lubricants from evaporating off. According to a jet propulsion lab technical memorandum, most of the actuators developed by them use greases and silicone oils. These are sealed using multiple O-rings. This setup is able to keep gas loss at $2 \times 10^{-5} \frac{\text{cm}^3}{\text{s}}$ at room temperature. This translates to a loss of 1 psi in pressure over 30 years. Greases also have lower evaporation losses and in the case of an O-ring failure they are able to keep the mechanism running for a little longer compared to oils [14].

2. Polymers and Space Environment

When choosing a material for the truss structure, the goal was to find a material that has good mechanical properties, easy to join, and will survive in Low Earth Orbit conditions. Polymers have great potential in the context of space applications due to weight savings and a variety of joining options [15]. Thermoplastics stood out as the best option compared to thermosets due to its high fracture toughness, damage tolerance, and weldability [16]. Materials in LEO cycle through a range of $-65 \text{ }^\circ\text{C}$ to $+125 \text{ }^\circ\text{C}$ [9] which can lead to the development of microcracks [17]. Cracks can also develop on the surface from the crosslinking of polymer surface due to solar ultraviolet radiation [17]. Corrosion from atomic oxygen is an additional element to consider [17]. Carbon fiber reinforced PEEK offers good resistance to thermally induced microcracking [17] and good resistance to degradation under radiation exposure [18]. PEEK is also one of the most resistant polymers to atomic oxygen [19]. To further support the case, PEEK is used as a primary

structure material for the articulated robotic arm on the ISS as well as on instruments like the Search-Coil Magnetometer which was part of the Parker Solar Probe Mission [20]. The combination of experimental data along with a record of space applications makes carbon fiber reinforced PEEK an ideal candidate for building trusses in space.

3. Joining

We considered many joining technologies, including laser welding, ultrasonic welding, mechanical fastening, adhesive bonding, snap fitting, and induction welding.

Laser welding has been used in space to weld stainless steel using a 38 W laser [21]. However, the power may range from 1 W – 100 W depending on the material and geometry [15]. Plastics can be combined with additives to aid in welding, but the plastics must be compatible with each other [15]. It is important to not let the laser over penetrate the welding joint [21].

Ultrasonic welding only generates heat near the welding zone [15]. Some other advantages of ultrasonic welding are that it requires no extra material [16], it has minimal off gassing [22], and it takes between 0.3 s – 3 s [23]. Its disadvantages are that it is limited in joint geometry [16], and it takes 1700 W – 5000 W of power to perform [23].

Using fasteners to join generates very little heat and allows for dissimilar materials to be joined [16]. However, there is a large stress concentration present, and it uses up more material than welding operations.

Adhesive bonding also allows for dissimilar materials to be joined and has negligible stress concentrations. However, adhesive bonding requires surface preparation and is weaker than using fasteners [16].

Snap fits are simple mechanical joints where two objects join by interlocking with each other [24]. Snap fits appeared to be a promising option due to its simplicity and the ability to assemble and disassemble quickly. However, snap fits are prone to stress concentrations due to their geometry [24] and their reliability in the harsh environment of space is questionable.

Induction welding uses an induction coil with an alternating current input to generate an electromagnetic field which is used to heat metallic implants in a plastic workpiece [25]. Compared to the other welding methods, this is a far simpler process, but the manufacturing of the beams will be more complicated. Using some equations from the Handbook of plastics joining [26], and using conservative parameters, we determined that it will take approximately 133 W to weld our beams in 1 s.

C. Iterations

1. Iteration 1

This design is the first design to be modeled in CAD. It includes components necessary to navigate a truss structure. The central bridge houses a ball screw driven by a stepper motor to facilitate the linear motion necessary to compress beams. The two hexagonal nexuses each house a central gear to rotate the robot, and a rack and pinion to move the torque arms axially. The rack is machined into the torque arm. The driving motors are present in the assembly, but not their respective pinions. The black collar present in Fig. 3 is to allow for the rotation of the torque arm, while keeping the nexus sealed.

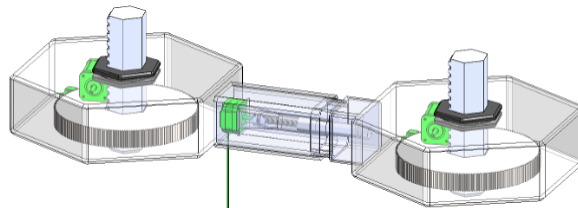


Fig. 2 Full assembly of the first iteration

The creation of this design served as a basis to eliminate flaws with the concept. For instance, the beam magazine needed to be designed such that it wouldn't be crushed when the compression operation occurs. This design also doesn't have a method of securing the nodes to the torque arm axially. The rack on the torque arm is exposed to space, which will lead to a rapid loss of lubrication, and eventually an early failure. These issues would be addressed in future designs. When installing the final beam in the triangular truss, two nodes must be spaced apart, which will create a bending load on the already installed beams.

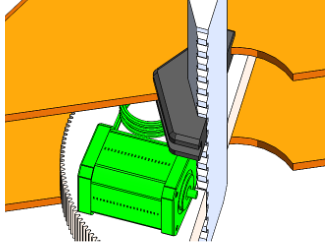


Fig. 3 View of the collar in the first iteration

2. Iteration 2.1

Iterations 2.1 and 2.2 were developed simultaneously to address problems present in the first iteration. They are both fully realized in terms of what motions they go through. However, there are no actuators present to produce these motions. Iteration 2.1 refines the execution present in the first iteration. Iteration 1 lacked any definition on how the beams and nodes that make up the truss will be dispensed. In iteration 2.1, in Fig. 4, magazines for the beams and nodes are added. The magazine for the nodes is integrated into the nexus housing where the motors that drive the torque arm are housed. The two halves of the bridge were integrated to both of the nexus and the magazine is solidly mount to the left nexus in dark green in Fig. 4. To transfer the beam from the magazine to the working area, an arm was added to the same nexus so that both the arm and the magazine move together.

The operation of this concept would start with the robot being attached to a node that is fixed to the payload area of the satellite. In essence, one of the nexuses is engaged with the node. A second node is dispensed and aligned by the other nexus and the arm pulls a beam from the beam magazine and aligns it with the nodes. The bridge section of the nexuses collapses and compresses the beam into the nodes. The beams are locked in place by means of a snap fit.

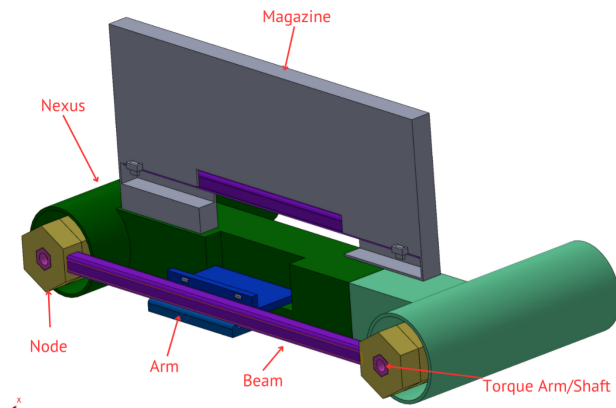


Fig. 4 Full assembly for iteration 2.1

To complete a triangular planar truss, this process can be repeated for a second time where the beam is oriented to 60 degrees from the first beam. However, a third beam cannot be placed without stretching the assembly of the three nodes and the two beams. The problem is that the beams are attached by sliding the beam into the nodes in the longitudinal axial direction. This is illustrated in Fig. 5.

This design also introduces modifications to the way the nexus operates. The torque arm serves double duty in this case. It aids in locomotion across the truss and as node magazine. The nexus housing is divided into two chambers in Fig. 5. One chamber houses the locomotion actuators, and the other one is a magazine for the nodes. The torque arm is located in the center (in pink). A plunger (in red) slides inside the torque arm and actuates four tabs which engage the torque arm to the nodes. The torque arm rotates about its longitudinal axis and translates in the direction of the same axis.

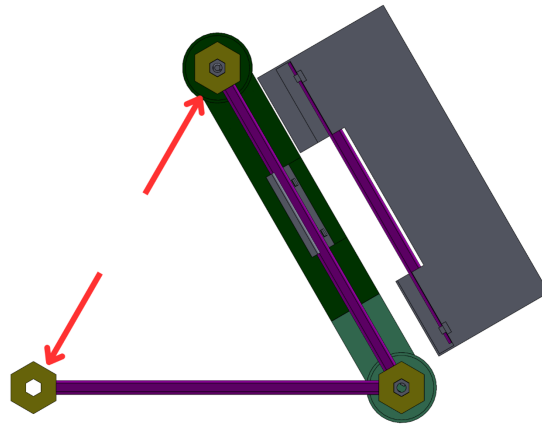


Fig. 5 Triangular truss partially assembled

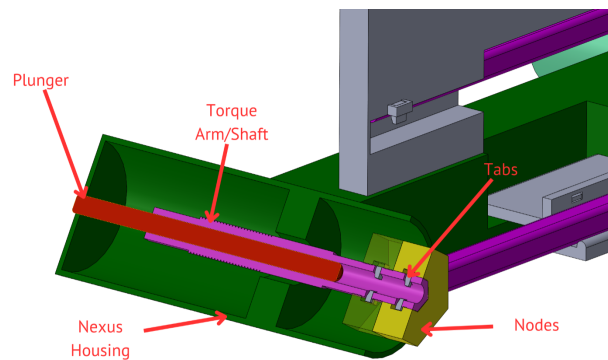


Fig. 6 Nexus cross sectional view

3. Iteration 2.2

Iteration 2.2, in Fig. 7, remains conceptually the same as Iteration 1, but the execution is unique. Instead of axially compressing the beams to engage a snap fit, a transverse load is applied to nodes which are open on one face. This feature allows for the bridge to be static, rather than being motorized.

The nodes are stored within each nexus, then pressed into place by the torque arm. The beam magazine translates downward to apply the force necessary to snap fit the beam to the node. The magazine makes use of an action bar and peg mechanism lock the beams in place while installing them. While this iteration is less complex than the alternatives, it has a significant flaw. Due to the nexus acting as a C-clamp to the node, it is not possible to create more than one triangle unless the robot swings around the outside, which itself would impose a significant size constraint, due to the nature of the payload volume.

4. Iteration 3

Iteration 3 is similar to Iteration 2.2, but the nexuses are modified to allow for the use of the node tabs concept from Iteration 2.1. The torque arms attach themselves to the nodes, then lower them below the robot. This adds some complexity, but it is necessary to navigate an entire truss.

5. Iteration 4

The primary goal of this iteration was to remodel the robot while accounting for the payload dimensions. 9 shows the size and shape of the beams and nodes. The extrusion near the end of the beams are present to minimize the axial

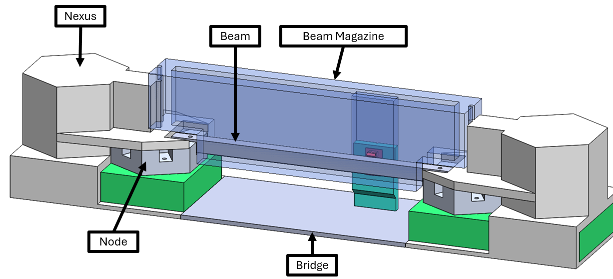


Fig. 7 Full assembly of iteration 2.2

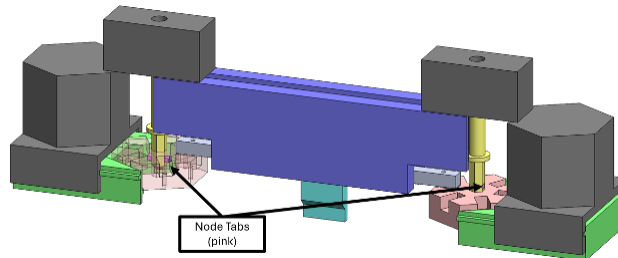


Fig. 8 Full assembly of iteration 3

load felt by the snap fit, although partway through this design's creation, ZES had decided to pursue the induction welding method. The induction coil will be mounted to the magazine. Additionally, the magazine locking mechanism was simplified to use a rotation input instead of the action bar.

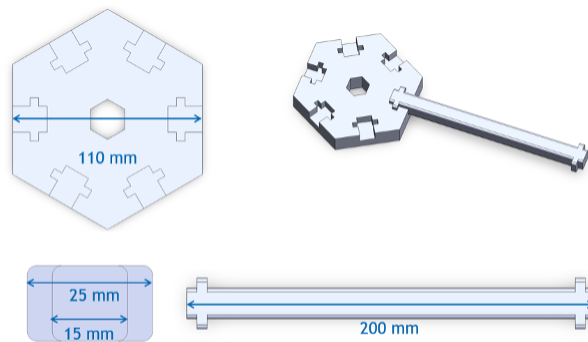


Fig. 9 Beam and node dimensions for iteration 4

The two nexuses that house the node magazine were tied using a cross bar. The beam magazine also interfaces with the cross bar using a sliding mechanism. The torque arm in figure 5 goes through the cross bar and is located between the magazine and the nexus in both sides (part in pink). The mechanisms that actuate the torque arm are all encased in the torque arm housing where they can be protected from the space environment. The torque arm is vertically actuated by a servo and a slider fork (red). The slot in the slider fork engages with the pegs on the hub (orange). This hub allows the torque arm to rotate freely about the longitudinal axis of the torque arm but constrains the vertical moment in the same axis. The rotation of the torque arm is controlled by a gear where the torque arm is free to slide through the gear.

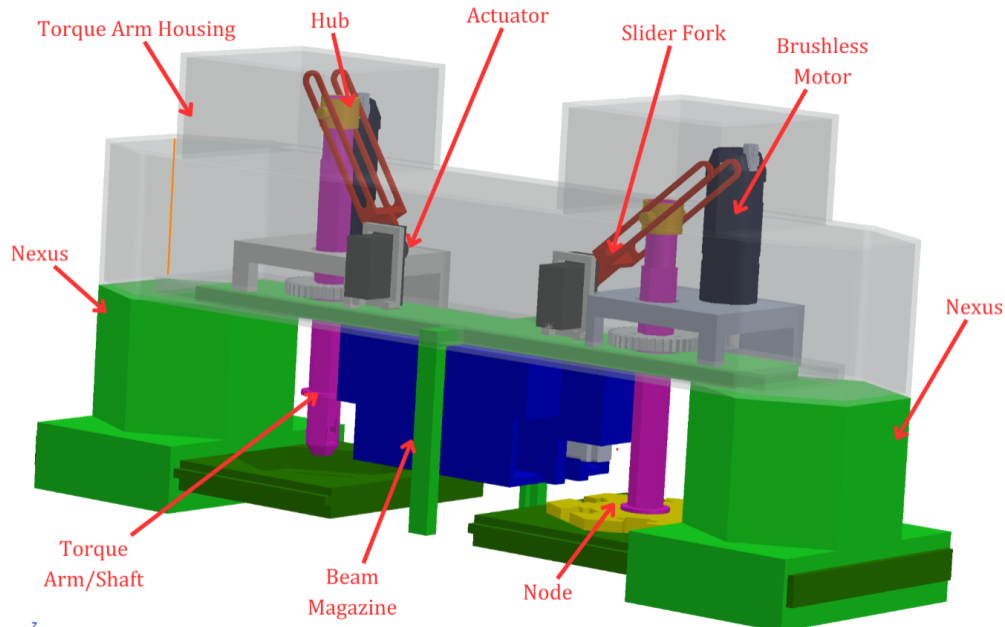


Fig. 10 Fourth iteration full assembly

D. Prototype Design

1. Motivation of Prototype

The use of a prototype seemed essential as all of the conceptual design was built from the ground up. Because of this, we sought to have a semi-fully functioning assembly of the AITAR to demonstrate all mechanical functions. The main goal of the prototype design is to demonstrate the sequencing between the beam magazine, node magazine, and torque arm.

2. The Process

Design of the prototype began with the selection of the motors needed for its construction and operation. Additionally, changes in scale were considered based off the sizing of the beams and nodes. At this point, the team was split into working groups based on the major subassemblies of the prototype: the beams and nodes, the beam magazine, the node magazine, and the torque arm. Each team would focus on building a workable digital model of their subassembly that was suited for printing and adjustable based on the requirements that would be imposed by interaction with other subassemblies.

Since this prototype was merely a proof of the mechanical concept, several adjustments were made to accommodate easier and cheaper construction. These changes included the substitution of built-in magnets rather than induction welding for connecting beams to node, the replacement of linear actuators with DC motors and gear mechanisms for driving the feeder tray, and the use of PLA rather than metal parts. As a result of the design process dividing the robot into subassemblies, rather than a specially designed and integrated bridge to connect all subassemblies, it was instead found most feasible to mount each piece individually at appropriate points along a $38\text{mm} \times 38\text{mm}$ aluminum extrusion.

In the initial conceptual design, both node and beam magazines were modelled as empty blocks, which could contain the parts they dispensed but had no features to actually dispense them. We selected 1.96lb constant force springs to provide force for the follower to push items down the magazine. The beam magazine was split into a shell with guide tracks for the follower, isolator modules for the separator pegs, the follower itself, and the mount for the linear screw to drive it into and out of the build plane. Two stabilizer rods were additionally added to prevent rotation or misalignment during this actuation. Most internal features were also given rounded edges to avoid catching during operation.

The node magazine added a single track for the spring to be placed within, and the follower featured two stacked sets of bearings to mitigate friction against the interior walls, as well as preventing it from changing angle inside the

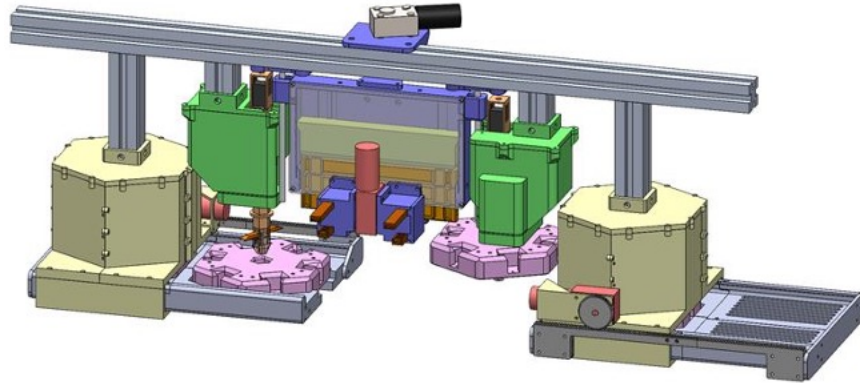


Fig. 11 Prototype digital twin

magazine. 12V 1.6A DC motors were selected for the linear actuation of the beam magazine, using a lead screw, and the feeder trays, using a rack and pinion mechanism offset to the side of the tray and mounted to the ends.

The torque arm faced the most initially demanding aspects of the design, needing to rotate, actuate in and out of the build plane, and extend the securing tabs. In order to avoid placing components inside a complex slip ring or restricting its rotation, the actuation for the tabs was moved into a nonrotating cab atop the arm. The two motors needed to lift and rotate the arm were placed within a housing module. Due to packaging restrictions inside the narrow volume of the torque arm, the linear peg design for securing nodes was replaced with rotating tabs. Additionally, due to insufficient holding force, the solenoid initially used to actuate the tabs was replaced with a pair of servo motors. A NEMA 17 stepper motor was selected to rotate the arm, a 25kg hobby servo motor was used for the lifting mechanism, and two RC toy servos were used for the tab actuation.

Early in the design process, we chose to scale up the beams for easier printing and to better house the magnets for the assembly sequence. These $6\text{mm} \times 2\text{mm}$ coin magnets were needed to attach the nodes to the beams and the feeder tray during operation regardless of orientation, as the force of gravity would otherwise cause the assembly to fall apart. Projections were added to the beams to secure them linearly, and matching cavities were added to the nodes. Rounded fillets were included on the contacting edges of both parts to allow them to slide into place. The central hole in the node was modeled based on hex socket heads to allow the torque arm to easily slide in as well. The diameter of the node varied during early design based on the required distance between the end of the magazine and the torque arm.

Many aspects of the prototype design were determined to be better than the conceptual design. When fabrication began, we noticed that the tabs used on the torque arm to arrest the nodes required more of a stroke length than necessary. They were then altered to allow a smaller stroke length from the actuator as well as adding the actuator to the main cab of the torque arm assembly instead of being in the bilge of the torque arm itself. This allowed us to use smaller actuators and ditch the complexity of the slip-ring that was required in the original conceptual design. We also fleshed out the design of the magazines, both node and beam, by adding constant force springs attached to followers. This change, plus some alignment alterations, allow the magazines to function properly and should be used in the design as this moved to the preliminary stages.

3. Next Steps

As the project passes onto the preliminary design stages, we have many recommendations for what should be implemented as well as things that should be improved upon. As mentioned above, the prototype design demonstrates more effective torque arm assemblies and magazine assemblies; these changes should be maintained as the project moves further.

There are recommendations that we have for design improvement, starting with the ability to autonomously reload the magazines. As it stands, there is no designed method for reloading truss elements by any method other than hand-installing; we do believe, however, that an autonomous solution is absolutely feasible and should be explored to add legitimate functionality of the design. Furthermore, we believe that the end walls of the beam magazine could be removed, allowing for the entire assembly to become modular and scalable. With the beam length no longer being

constrained by the assembly and instead just the width, beams of any reasonable size could be used for trusses. This is very feasible seeing as the node magazine and torque arm assembly only interface with the nodes themselves; the addition of this change would allow the robot to adapt to almost any structure requirements mission to mission with the only change in between being the spacing of the assemblies on the bridge.

IV. Analysis

A. Torque Arm Analysis

The locomotion of the robot is controlled via the torque arm which engages with the nodes and the robot turns about this torque arm. In microgravity, most of the expected forces on the torque arm are torsional where the robot swings about the torque arm. The moment of inertia about the pivot axis of the torque arm was found to be approximately $0.629 \text{ kg} \cdot \text{m}^2$. This property was found by applying Aluminum 2024 to all of the components in SolidWorks and reading values from the moment-of-inertia tensor about the torque arm axis. It was assumed that the maximum angular acceleration would be $10 \frac{\text{rad}}{\text{s}^2}$, and with all these values known. Eq. 1 can be used to solve for total torque required about the torque arm axis.

$$T = I\alpha \rightarrow [0.629 \text{ kg} \cdot \text{m}^2] [10 \frac{\text{rad}}{\text{s}^2}] = 6.29 \text{ N} \cdot \text{m} \quad (1)$$

Using the Ansys structural simulation system, this moment was applied to the torque arm in the area where it interfaces with the gear that rotates it. This can be seen in figure 12. The displacement constraints on the torque arm are applied in the features where the torque arm interfaces with the node (labeled as A and B).

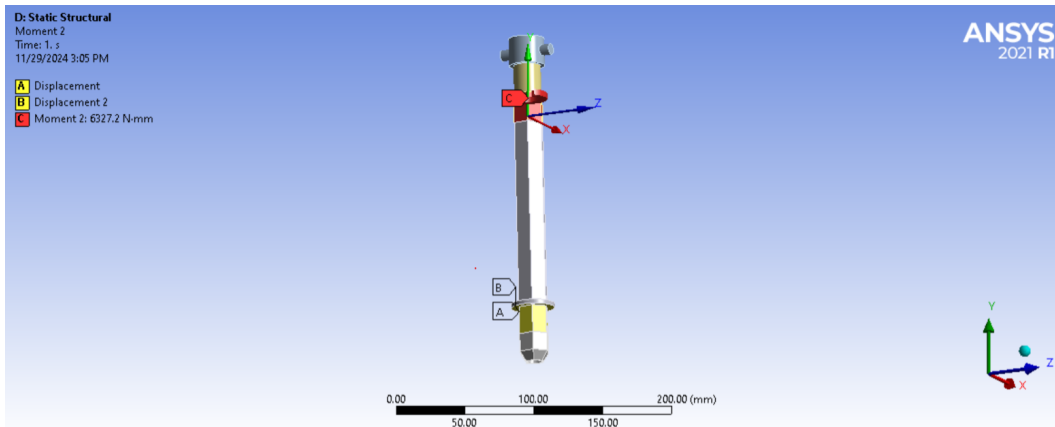


Fig. 12 Constraints and forces on the torque arm.

The equivalent stress and factor of safety for the torque arm (Al-2024) are the solutions of interest. For the torque arm, the maximum von-mises equivalent stress was to be 9.2 MPa and a minimum factor of safety that exceeds the ceiling that Ansys allows, both plots are shown in Fig. 13. This means the torque arm may be overbuilt for the expected torques. This is far from a problem when it comes to conceptual design as we are already within mass constraints. Removing material to allow a more efficient design is an process that falls within preliminary design, therefore outside of the scope of this project.

B. Gear Motor Sizing

With the torque required to move the arm determined, the next logical step is to determine how to apply this torque. We decided that a brushless DC motor with an encoder mechanically constrained would be the best option for this task. A stepper motor was also considered for this job, however we determined that this would be less viable for the application because of the low amount of torque that stepper motors can generate compared to their volume. Also, speaking to an expert on the matter Dr. Thomas Allsup, he had recommended that we avoid steppers because of the open-loop control scheme that steppers use. If this were to be tweaked in any way, the entire mission could fail just

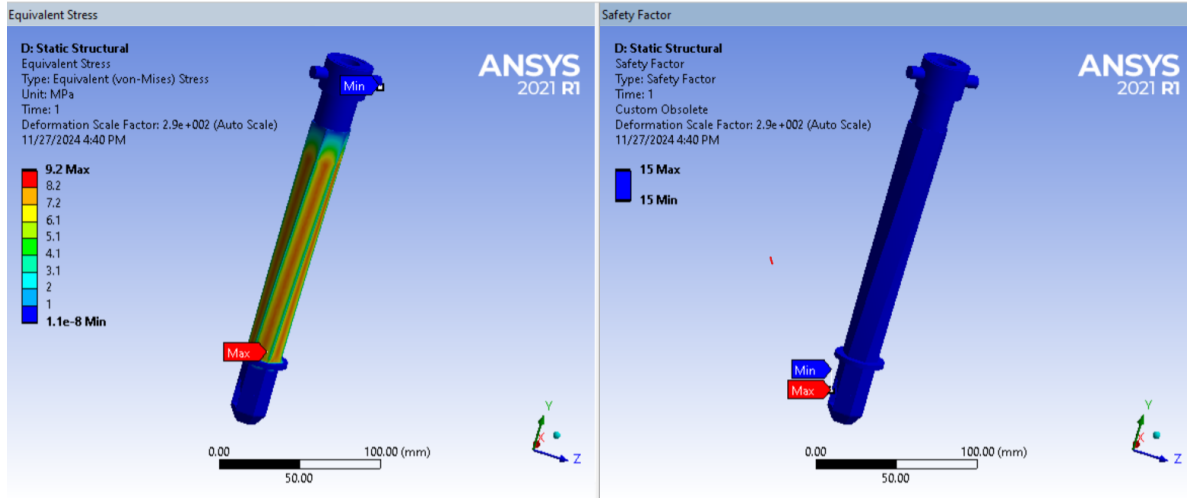


Fig. 13 Torque arm FEA

based on the motor no longer having proper understanding of where it is positioned. For this reason, a mechanically constrained encoder was chosen so that constant feedback can be gained.

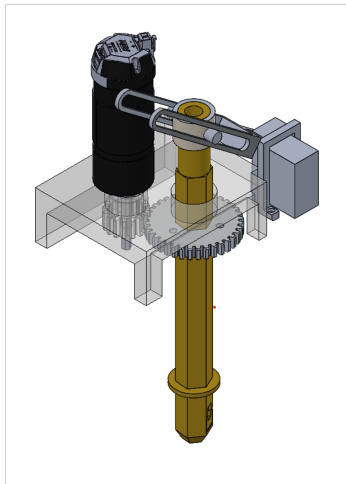


Fig. 14 Full torque arm assembly

Figure 14 shows the entire torque arm assembly including the gearing that will allow the rotational motion of the motor to transfer into the robot assembly itself. The motor was specced with an understanding of this step-down ratio, the entire process is shown in Eqs 2 and 3.

$$\frac{T_G}{T_P} = \frac{N_G}{N_P} \quad (2)$$

$$T_P = \frac{N_P}{N_G} I \alpha \rightarrow \frac{16}{36} [0.629 \text{ kg} \cdot \text{m}^2] [10 \frac{\text{rad}}{\text{s}^2}] = 2.8 \text{ N} \cdot \text{m} \quad (3)$$

C. Launch Analysis

In order to perform the launch analysis, research was done to determine expected launch accelerations as this will be the majority of the problem regarding launch anyway. We have found that, during launch, we can expect accelerations

up to 6 G's commonly. An Ansys simulation was used to determine maximum equivalent stress of the assembly at 6 G's of acceleration. The results of which are shown in Fig. 15

The simulation was set up with a quadratic mesh of 3 mm and 6 G's of inertial loading applied in the appropriate direction. We made an assumption regarding the supports and applied a remote displacement support on both sides of the nexus platforms to simulate a sort of bracket on either end that will secure the robot to the bus. Some problems were encountered regarding the mesh sizing for the complex torque arm assembly with the gearing; because of this, we made a conservative estimate by calculating the mass with SolidWorks and applying the appropriate force ($F = MA$). The results show that the maximum stress that the robot experiences is 13 MPa, far from anything that would be worrying.

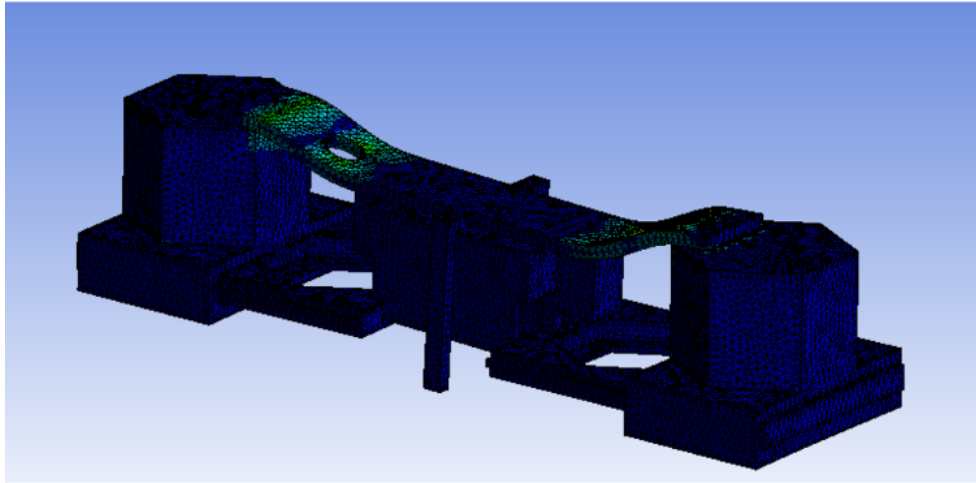


Fig. 15 Graph of equivalent stress for launch conditions

V. Conclusion

The group created a conceptual design for an Autonomous In-space Truss Assembly Robot and developed that design into a prototype demonstrating its fundamental mechanical operations. This concept was chosen by the group as a response to the COSMIC Consortium's C3 Capstone competition, requiring design for an ISAM mission performed using at least three operations and launched in the payload space of the BCT Venus-class bus. Other diverse concepts were studied, including debris stabilization, debris recycling, solar panel repair, and new 3d printing techniques. Truss assembly was chosen due to its feasibility, utility, and compelling design challenges. The final conceptual design loads truss nodes onto its actuated torque arms to position them within the build plane, then lowers its beam magazine into position to deposit beams into the nodes and weld them in place via induction coils. Once a portion of the truss is complete, the robot can then locomote along it using the same torque arm mechanism as was used to position the node. Construction of the physical prototype has allowed for refinement of the operational principles and shows clear areas where the concept can be improved. The design can be made more flexible by altering the magazine design to accept multiple beam lengths, as well as including mechanisms to allow the reloading of beams. Through this process, we have determined that, with proper design touch-ups and testing, that this conceptual design can function and be implemented into future missions within the decade.

References

- [1] Anderton, D. A., “Space Station,” 1985.
- [2] Corp., S. E. T., “Rideshare Payload User’s Guide,” 2024.
- [3] Nwokocha, F., Zagrai, A., and Anderson, M., “EFFECT OF SPACE ENVIRONMENT ON STRUCTURAL DIAGNOSTICS,” *Proceedings of the 14th International Workshop on Structural Health Monitoring*, Destech Publications, Inc., Sept. 2023.
- [4] “Large Constellations of Satellites: Mitigating Environmental and Other Effects,” 2022.
- [5] “Geostationary Orbit,” https://www.esa.int/ESA_Multimedia/Images/2020/03/Geostationary_orbit.
- [6] Guardabasso, P., Skoulidou, D. K., Bucci, L., Letizia, F., Lemmens, S., Ansart, M., Roser, X., Lizy-Destrez, S., and Casalis, G., “Analysis of Accidental Spacecraft Break-up Events in Cislunar Space,” *Advances in Space Research*, Vol. 72, No. 5, Sept. 2023, pp. 1550–1569.
- [7] Thomas, A., Green, D., Ammons, K., Jalil, L., Kusters, J., and Cahoy, K., “Protecting Satellites in Low Earth Orbit: An Overview of Hazards and Policy Solutions,” *MIT Science Policy Review*, Vol. 4, Aug. 2023, pp. 67–75.
- [8] J.W. Howard, Jr., D. H., “Spacecraft Environments Interactions- Space Radiation and Its Effects on Electronic Systems,” 1999.
- [9] Plante, J. and Lee, B., “Environmental Conditions for Space Flight Hardware - A Survey,” .
- [10] Wang, J. T., “Cold- Welding Test Environment,” .
- [11] Waddell, T., Toombs, J., Reilly, A., Schwab, T., Castaneda, C., Shan, I., Lewis, T., Mohnot, P., Potter, D., and Taylor, H., “Use of Volumetric Additive Manufacturing as an In-Space Manufacturing Technology,” *Acta Astronautica*, Vol. 211, Oct. 2023, pp. 474–482.
- [12] “Low Earth Orbit Visualization | LeoLabs,” <https://platform.leolabs.space/visualization>.
- [13] Vest, C. E., “LUBRICATION OF SPACECRAFT MECHANISMS,” .
- [14] FORNIA, CALI., “JET PROPULSION LABORATORY,” 1972.
- [15] Humbe, A. B., Deshmukh, P. A., Jadhav, C. P., and Wadgane, S. R., “REVIEW OF LASER PLASTIC WELDING PROCESS,” .
- [16] Bhudolia, S. K., Gohel, G., Leong, K. F., and Islam, A., “Advances in Ultrasonic Welding of Thermoplastic Composites: A Review,” *Materials*, Vol. 13, No. 6, March 2020, pp. 1284.
- [17] Silverman, M., “Space Environmental Effects on Spacecraft: LEO Materials Selection Guide,” .
- [18] Garvey, R., “Potential for Advanced Thermoplastic Composites in Space Systems,” 1990.
- [19] Esha and Hausmann, J., “Material Characterization Required for Designing Satellites from Fiber-Reinforced Polymers,” *Journal of Composites Science*, Vol. 7, No. 12, Dec. 2023, pp. 515.
- [20] Rival, G., Dantras, É., and Paulmier, T., “Ageing of PEEK/Carbon Fibre Composite under Electronic Irradiations: Influence on Mechanical Behaviour and Charge Transport,” *Composites Part A: Applied Science and Manufacturing*, Vol. 154, March 2022, pp. 106769.
- [21] N. Naden, T. P., “A Review of Welding in Space and Related Technologies,” 2020.
- [22] Miller, S., Pinakidis, J., Bryant, R., Lang, C., Bergan, A., and Segal, K., “Innovations in Continuous Ultrasonic Welding of Thermoplastic Composites and Evaluation for Space Applications,” .
- [23] Li, H., Chen, C., Yi, R., Li, Y., and Wu, J., “Ultrasonic Welding of Fiber-Reinforced Thermoplastic Composites: A Review,” *The International Journal of Advanced Manufacturing Technology*, Vol. 120, No. 1-2, May 2022, pp. 29–57.
- [24] Jmerson, L., “Design Guide for Snap-Fits | Product Design Series,” May 2024.
- [25] Troughton, M. J., “Handbook of plastics joining: a practical guide,” Vol. 2, No. 11, 2008, pp. 113–120.
- [26] Ahmed, T., Stavrov, D., Bersee, H., and Beukers, A., “Induction Welding of Thermoplastic Composites—an Overview,” *Composites Part A: Applied Science and Manufacturing*, Vol. 37, No. 10, Oct. 2006, pp. 1638–1651.